Characterization of Ordered Mesoporous Carbons Synthesized Using MCM-48 Silicas as Templates

Michal Kruk and Mietek Jaroniec*

Department of Chemistry, Kent State University, Kent, Ohio 44242

Ryong Ryoo and Sang Hoon Joo

Department of Chemistry and School of Molecular Science (BK21), Korea Advanced Institute of Science and Technology, Taejon, 305-701 Korea

Received: March 6, 2000; In Final Form: June 9, 2000

CMK-1 ordered mesoporous carbons were synthesized using MCM-48 silica templates with a wide range of unit-cell parameters and pore sizes. Sucrose and furfuryl alcohol were employed as carbon precursors. It was confirmed that the isolation of the CMK-1 carbon via dissolution of the MCM-48 template is accompanied by a structural transformation, which manifests itself in the change of the X-ray diffraction pattern. It is suggested that the transformation is related to the disconnected nature of the two interwoven parts of the CMK-1 framework (which are formed in two enantiomeric MCM-48 channel systems separated by the silica wall) and may involve a mutual displacement of these two parts to create some contact between them and fix their mutual position. It was shown that the application of different MCM-48 templates allowed for tailoring of the CMK-1 unit-cell size. However, the primary mesopore size of CMK-1 was found to be relatively constant. This was explained as a consequence of the formation of primary mesopores of CMK-1 in the space previously occupied by the MCM-48 pore walls, and attributed to the similarity in the pore wall thickness for the MCM-48 templates used. Our study confirmed that the uniform mesopores of CMK-1 are accompanied by micropores and that the carbon prepared using MCM-41 as a template collapses upon the template removal to yield high-surface-area disordered microporous structure. It was also shown that thermogravimetric weight loss behavior under air atmosphere provides important insights to the structural integrity and quality of the CMK-1 samples.

1. Introduction

Porous carbons are commonly used as adsorbents and catalyst supports.[1,2] While many porous carbons are known to exhibit periodic structures resulting from the uniform stacking of graphene sheets and periodic arrangement of atoms within these sheets,[1,2] carbons with periodic porous structures have been reported only recently. Some carbons, such as fullerenes or single-wall nanotubes (SWNTs), exhibit periodic structures[3,4] with voids potentially accessible to some adsorbate molecules. Moreover, SWNTs can be opened, thus rendering their interiors accessible to adsorbate molecules.[5−8] However, the periodically arranged fullerenes and SWNTs are held together via weak van der Waals interactions,[3,4] so these materials cannot be considered as systems with permanent ordered porosity. Macroporous carbons with periodic inverse opal structures were reported recently,[9] but the employed approach based on the templating with porous silica opal crystals cannot be readily generalized on the synthesis of carbons with periodic mesoporous or microporous systems. It should be noted that macropores, mesopores, and micropores are defined here as pores of the width above 50 nm, between 2 and 50 nm, and below 2 nm, respectively.[10] Zeolitic templates with periodic microporous structures were also employed in the carbon synthesis, but in this case, the ordering characteristic of the template was lost upon its dissolution necessary to obtain the porous carbon structure.[11−13] Apparently, carbon frameworks formed in narrow pores of zeolites were not rigid enough to retain periodicity, although their integrity and structure were often retained to such an extent that the templated carbon particles exhibited the morphology of the zeolite template particles.[11−13] Moreover, the zeolite-templated carbons had large specific surface areas and micropore volumes,[11−13] without activation usually required to develop an accessible microporous structure.[11]

The discovery of ordered mesoporous materials[14] opened new opportunities in the synthesis of periodic carbon structures using the templating approach. In particular, the use of MCM-48 silica[14,15] allowed for the preparation of the first carbon with a periodic framework of the unit-cell size of several nanometers.[16] This material, designated as CMK-1, exhibited high specific surface area, arising from the presence of uniform mesopores of the width about 3 nm and micropores. A periodic mesoporous carbon was also obtained using SBA-1 silica as a template.[16] Later, an ordered mesoporous carbon analogous to CMK-1 was synthesized by others;[17] a high-surface-area mesoporous carbon (designated as SNU-2) was obtained[18] using disordered HMS siliceous molecular sieve,[19] whereas MCM-41 template[14] was found to be unsuitable for the preparation of a mesoporous carbon.[18] Both CMK-1 and SNU-2 carbons were shown to exhibit facile properties as electrochemical double-layer capacitors.[17,18] One can also envision applications of ordered mesoporous carbons as catalyst supports, adsorbents, sensors, and

* Corresponding author. Tel. (330) 672 3790. Fax (330) 672 3816. E-mail: jaroniec@columbo.kent.edu.

10.1021/jp000861u CCC: $19.00
Published on Web 07/20/2000

electrode materials.[16] The simplicity of the synthesis of the mesoporous carbons[16] as well as the recent development of facile methods for the synthesis of MCM-48 templates[20,21] and the ease of synthesis of HMS templates[19] open an opportunity for the large-scale production of these novel carbons.

The current study provides a comprehensive description of structural properties of CMK-1 carbons, describes the relation between the structure of MCM-48 template and the resulting CMK-1 material, and suggests a methodology for quality control of CMK-1 materials using thermogravimetry.

2. Materials and Methods

2.1. Materials. MCM-48 silicas were synthesized using alkyltrimethylammonium/cosurfactant mixtures as described elsewhere.[20,21] The samples templated by alkyltrimethylammonium with the alkyl chain length of *n* carbon atoms ($n = 12$, 14, 16, 18, and 20) are denoted C*n*-MCM-48. MCM-41 silica was synthesized as reported earlier[22] using a mixture of cetyltrimethylammonium and cetyltriethylammonium surfactants. The detailed characterization of MCM-41 prepared under these conditions was reported elsewhere.[23] Porous carbons templated by MCM-48 and MCM-41 were obtained using a recently reported procedure involving impregnation with sucrose in the presence of sulfuric acid, followed by carbonization at 1173 K and removal of the silica template via dissolution in NaOH solution.[16] Carbons prepared using C*n*-MCM-48 and MCM-41 templates are denoted C*n*-CMK-1 and C-41, respectively. An ordered carbon molecular sieve (denoted as CMK-1-FA) was also prepared using furfuryl alcohol as a carbon precursor.[16] In this case, C16-MCM-48 silica was converted to the aluminosilicate form using a postsynthesis alumination method,[24] and sulfuric acid was not used. In addition, a carbon sample (denoted as C-sucrose) was prepared from sucrose under the same conditions as described above but without using a silica template.

2.2. Methods. Powder X-ray diffraction (XRD) patterns were recorded on a Rigaku D/MAX-III diffractometer using Cu Kα radiation. Nitrogen adsorption isotherms were measured on a Micromeritics ASAP 2010 volumetric adsorption analyzer. Before the adsorption measurements, the samples were outgassed for 2 h at 473 K in the degas port of the adsorption analyzer. Weight change curves were recorded on a TA Instruments TGA 2950 high-resolution thermogravimetric analyzer using a high-resolution mode. Runs under nitrogen and air atmospheres were carried out using maximum heating rates of 5 and 20 K min^{-1}, respectively. The ash content was evaluated from the residue at 1260 K after runs under air atmosphere. Since the ash content for the templated carbons was found to be relatively small, a blank determination of the weight change for an empty platinum pan was carried out and the residue amounts for the carbons were corrected accordingly (the corrections were below 0.5% of the weight loss for CMK-1 sample). The percentage of carbon in the carbon−silica composite materials was estimated from the thermogravimetric weight loss in air between 373 and 973 K. In this temperature range, the silica templates calcined at 823 K exhibited weight loss of about 1%, so the error in the carbon content evaluation related to the dehydroxylation of the silica component of the carbon−silica composite is expected to be below 1%.

2.3. Calculations. The BET specific surface area[10] was calculated from the nitrogen adsorption data in the relative pressure range from 0.04 to 0.2 for silicas and from 0.04 to 0.1 for carbons. In the latter case, the range was narrower, because the ordered carbon molecular sieves exhibited capillary condensation at relative pressures lower than those for the silica templates. The total pore volume[10] was evaluated from the amount adsorbed at a relative pressure of 0.99. The primary pore volume and the external surface area were assessed by employing the α_s plot method.[10,25−27] Silica[27] and nongraphitized carbon[26] reference adsorption isotherms were used for the silicas and carbons, respectively. The secondary pore volume (that of pores wider than the primary pores, but still detectable by nitrogen adsorption, that is of the width between about 5 and 200−400 nm) was determined as a difference between the total pore volume and the primary pore volume. In the case of MCM-48 and MCM-41, the determined primary pore volume provides exclusively the volume of the primary (ordered) mesopores, but in the case of carbons, it also includes contribution of the micropore volume. The α_s plot calculations were performed in the standard relative adsorption, α_s, range of 1.5−2.0 for carbons; 1.3−1.7 for C14-, C16-, and C18-MCM-48; 1.6−2.0 for C12-MCM-48 and MCM-41; and 1.5−2.1 for C20-MCM-48 (α_s is defined as the amount adsorbed at a given relative pressure divided by the amount adsorbed at a relative pressure of 0.4). The micropore volume for the silica templates was calculated from the data in the α_s range from 0.0 to 0.7. The primary mesopore size of the silica templates and carbon molecular sieves was evaluated using the Kruk−Jaroniec−Sayari (KJS) approach[28] and the calculation procedure based on the concept of Barrett, Joyner, and Halenda (BJH),[29] but without the simplifying assumptions employed by the latter authors. Although it was demonstrated that the accuracy of this pore size evaluation procedure is very good even for materials with surface properties different from those of the silicas used for the calibration of the KJS procedure,[30] the employed assumption of the cylindrical pore geometry may render this method inaccurate for the CMK-1 ordered carbon molecular sieves. Therefore, the primary mesopore size of the CMK-1 samples was also evaluated using the DFT Plus software developed for carbons with slitlike pore geometry.[31] The pore wall thickness, *b*, for MCM-48 was calculated as proposed by Ravikovitch and Neimark[32] using an equation based on the pore volume:

$$b = \left(1 - \frac{V_p \rho}{1 + V_p \rho}\right)\frac{a}{x_0} \qquad (1)$$

where ρ is the pore wall density (assumed to be 2.2 g cm^{-3}),[32−34] *a* is the unit-cell size of MCM-48 (calculated from (211) interplanar spacing d_{211}: $a = 6^{1/2}d_{211}$), and x_0 is a constant ($x_0 = 3.0919$). The pore wall thickness for MCM-41 was calculated from the XRD (100) interplanar spacing and the primary mesopore volume as described elsewhere, assuming hexagonal pore geometry.[23,34]

3. Results and Discussion

3.1. MCM-48 and MCM-41 Templates. The results of XRD, nitrogen adsorption, and TGA characterization of the C20-MCM-48 silica used in the current study have already been reported elsewhere.[21] The structural properties of the other MCM-48 samples were in general similar to those for the corresponding samples studied in refs 20 and 21, although C12-MCM-48 sample used in the current work had somewhat larger pore size, surface area, and primary mesopore volume as well as lower secondary mesopore volume (difference between the total pore volume and the primary mesopore volume). The MCM-41 sample used was similar to C16 MCM-41 sample described in ref 23, but had significantly lower secondary pore

TABLE 1: Structural Properties of MCM-48 and MCM-41 Silica Templates and Silica/Carbon Composite Materials[a]

sample	a (nm)	S_{BET} ($m^2\ g^{-1}$)	V_t ($cm^3\ g^{-1}$)	V_p ($cm^3\ g^{-1}$)	S_{ex} ($m^2\ g^{-1}$)	w_{KJS} (nm)	b (nm)	C[b] (%)	SiO_2[b] (%)
C20-MCM-48	10.92	1130	1.46	1.14	110	4.53	1.01	37	55
C18-MCM-48	10.17	1140	1.25	1.05	90	4.15	0.99	38	55
C16-MCM-48	9.60	1130	1.20	0.99	100	3.97	0.98	37	59
C14-MCM-48	9.33	1100	1.00	0.88	70	3.71	1.03	38	54
C12-MCM-48	9.21	1150	1.02	0.96	40	3.68	0.96	35	60
MCM-41	4.62	1100	0.93	0.88	30	3.81	0.87	36	58

[a] a, XRD unit cell parameter equal to $6^{1/2}d_{211}$ for MCM-48 and $2\cdot3^{-1/2}d_{100}$ for MCM-41; S_{BET}, BET specific surface area; V_t, total pore volume; V_p, primary pore volume; S_{ex}, external surface area; w_{KJS}, primary mesopore diameter; b, pore wall thickness; C, percentage of carbon estimated from the TGA weight loss between 373 and 973 K under air atmosphere; SiO_2, percentage of silica estimated as the TGA residue at 1260 K under air atmosphere. [b] Data for silica/carbon (silica = MCM-48 or MCM-41) composite materials.

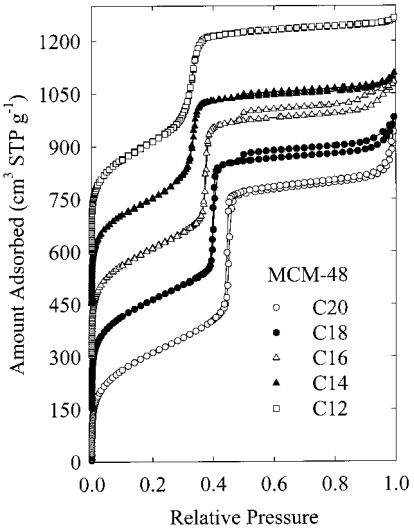

Figure 1. Nitrogen adsorption isotherms for the MCM-48 templates. The adsorption data for C18-, C16-, C14-, and C12-MCM-48 were offset vertically by 150, 300, 450, and 600 cm^3(STP) g^{-1}, respectively.

volume. Selected structural properties of the silica templates are listed in Table 1. The XRD patterns of the MCM-48 and MCM-41 samples were characteristic of highly-ordered periodic materials. The MCM-48 silicas exhibited a wide range of unit cell sizes (from 9.2 to 10.9 nm) and primary mesopore sizes (from 3.7 to 4.5 nm). Their primary mesopore volumes and total pore volumes tended to increase as the alkyl chain length of the cationic surfactant used for their synthesis increased, although the primary mesopore volume of C12-MCM-48 was larger than that for C14-MCM-48. The pore size and pore volume of the MCM-41 sample were close to those of C14-MCM-48. The BET specific surface areas of the templates were in all cases very similar (about 1100 $m^2\ g^{-1}$). As can be seen in Figures 1 and 2, nitrogen adsorption isotherms for the silica templates featured narrow capillary condensation steps, especially for MCM-41 and C20-, C18-, and C16-MCM-48, indicating the high degree of pore size uniformity. Adsorption isotherms for C20-, C18-, and C16-MCM-48 exhibited hysteresis loops related to capillary condensation in secondary mesopores at relative pressures above about 0.5. As discussed elsewhere,[21] the secondary mesoporosity of calcined MCM-48 prepared under the synthesis conditions employed herein resembles that of the uncalcined material and therefore is primarily attributable to the presence of voids or imperfections within the structure of MCM-48 particles. The silica templates did not have any micropores, as shown from the α_s plot analysis.

3.2. Carbon−Silica Composites. In accord with the previous studies,[16,18] the carbon−silica composite materials exhibited XRD patterns characteristic of the silica support used for their preparation, although the intensities of the XRD peaks were

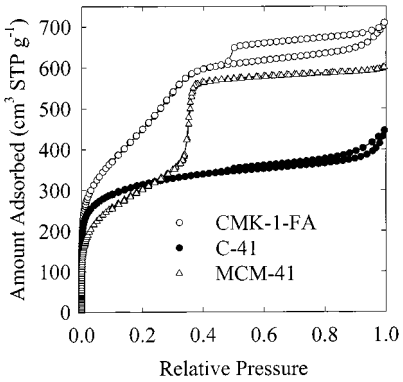

Figure 2. Nitrogen adsorption isotherms for the MCM-41 silica, CMK-1-FA carbon, and MCM-41-templated carbon.

much lower. The unit-cell parameters for the C*n*-MCM-48/carbon composites were 9−13% lower than those for the corresponding silica templates. Nitrogen adsorption provided a confirmation that the composites were microporous[16] (the micropore volume between about 0.1−0.2 $cm^3\ g^{-1}$ for MCM-48-templated composites and about 0.04 $cm^3\ g^{-1}$ for the MCM-41-templated composite), but in most cases, it was difficult to acquire fully reliable nitrogen adsorption data because of two reasons. First, the maximum measurement time for our adsorption analyzer (about 60 h) was insufficient to collect fully equilibrated adsorption data for most of the samples (except for those synthesized using C18- and C20-MCM-48 templates). Second, because of the slow equilibration, small sample sizes had to be used, which, combined with the relatively low external surface areas of these materials, made the evaluation of adsorption in the high-pressure range less reliable. For all the carbon−silica samples, low-pressure hysteresis[35] was observed, whose extent in general increased as the pore size of the silica template decreased. The sluggish equilibration and low-pressure hysteresis are indicative of poor accessibility of the pores (in this case micropores) in the structure. This in turn suggests that the micropores may have constrictions of the width comparable to the size of nitrogen molecule.[35] In such a case, there is also a distinct possibility that not all of the micropores present were accessible to nitrogen, because they might be too narrow or not connected with the exterior of the particles in such a way that nitrogen molecules could diffuse inside them. The observed micropores may be located within the carbon framework and/or between the silica pore walls and the carbon. It is also interesting that the templates with larger pore sizes afforded composites with better micropore accessibility. One can hypothesize that this is a result of more facile development of the micropore structure in wider voids of the template. Alternatively, if there are voids between the template and carbon within the structure, they may be wider and more easily accessible in the case where the pores of the template are wider.

For the silica/carbon composites, no steps were observed on their nitrogen isotherms in the pressure range of capillary condensation in primary mesopores of the templates, which indicates that these pores were essentially fully filled or blocked by the carbon deposit. The high-pressure hysteresis loops on the adsorption isotherms were similar to those for the templates, thus indicating that the carbon infiltration did not lead to any significant changes in the secondary porosity of the templates.

TGA under air atmosphere was used to determine the carbon and silica contents in the composite materials (see Table 1). The weight loss at temperatures below 373 K amounted to 4−8% and can be related primarily to the thermodesorption of physisorbed water. A major weight loss was centered in all cases at about 813 K and can be attributed to the combustion of carbon. Only a very small weight loss was observed at temperatures above 973 K, indicating that the combustion was essentially complete at the latter temperature.

As seen from Table 1, the composites exhibited the carbon/silica weight ratios between 0.58:1 and 0.70:1. Taking into account the absolute density of porous carbon (usually between 2 and 2.1 g cm^{-3};[2] the value of 2.05 g cm^{-3} is assumed in the current study) and the primary mesopore volumes of the silica templates (about 1 cm^3 g^{-1}), these carbon/silica weight ratios appear to be rather low. However, it needs to be kept in mind that the silica template shrinks considerably during the preparation of the carbon−silica composites, which involves the treatment at 1173 K, which is necessary to complete the carbonization step. To examine the resulting changes in the MCM-48 structure, carbon from a carbon/silica composite was removed via calcination. MCM-48 material was recovered with the unit-cell size similar to that of the carbon/silica composite, and significantly smaller than that of the MCM-48 material before carbon infiltration. The intensity of XRD reflections for the initial and recovered MCM-48 samples were similar (see Figure 1S, Supporting Information), which proves the retention of the structural integrity of the MCM-48 template during the carbon infiltration. These results are consistent with our findings that MCM-48 silica is stable in concentrated acids even under heating.

Let us assume that the silica template does not dissolve to any appreciable extent during the impregnation with sucrose and sulfuric acid, and the density of the silica template framework does not change during the impregnation/carbonization process and is equal to that of amorphous silica[33] (that is 2.2 g cm^{-3}). In such a case, the unit-cell parameter decrease observed (9−13%) would lead to a dramatic decrease in the volume of channels within the silica framework, since the corresponding reduction of the unit-cell volume would be 25−35% (shrinkage takes place in three dimensions) and the resulting smaller unit cell would contain the unchanged volume of the silica framework. In the case of the MCM-48 and MCM-41 samples under study, the resulting volume of channels within the silica framework (per 1 g of silica) would be reduced to 49−64% of the primary mesopore volume for the calcined silica templates. A similar magnitude of the pore volume (or adsorption capacity) decrease has already been reported for MCM-41 calcined at 1123−1273 K,[36−38] which was accompanied by a significant structural shrinkage.[37] The significant reduction of the template pore volume partially explains why the amounts of carbon in the carbon−silica composites were relatively low. Furthermore, as discussed above, adsorption measurements provided evidence of the presence of micropores either within the carbon framework formed or between the carbon and silica framework. It is interesting that on the basis of the considerations presented above, one can quite accurately predict the micropore volume of the carbon/silica composites. For instance, let us consider the evolution of the structure of a CMK-1 sample prepared using the C18-MCM-48 template. The volume occupied by 1 g of the MCM-48 primary mesopore structure is equal to the primary mesopore volume plus the volume of the siliceous pore walls: 1.05 cm^3 g^{-1} + 1/(2.2 g cm^{-3}) = 1.50 cm^3 g^{-1} (all volumes are rounded to the nearest 0.01 cm^3 g^{-1}). As a result of the structural shrinkage upon calcination, the volume corresponding to 1 g of the template is reduced to 1.05 cm^3 g^{-1} (that is, 1.50 cm^3 g^{-1}·[(9.01 nm)/(10.17 nm)]^3, where the last term provides the ratio of the unit-cell sizes after and before carbonization). This reduced volume still comprises the same (or highly similar) volume of silica, since the density of amorphous silica is relatively independent from the conditions of its preparation.[33] Therefore, the volume of pores confined within the silica framework is reduced to 1.05 cm^3 g^{-1} − 1/(2.2 g cm^{-3}) = 0.59 cm^3 g^{-1}. This volume is partially occupied by the carbon framework formed. 1 g of the carbon/silica composite contains about 55% of silica (this corresponds to the pore volume of 0.59 cm^3·55% = 0.32 cm^3) and about 38% of carbon, which occupies the volume of 0.38 g/2.05 g cm^{-3} = 0.19 cm^3. Therefore, the volume of micropores per gram of this carbon/silica composite is estimated to be about 0.32 − 0.19 cm^3 = 0.14 cm^3, which is in acceptable agreement with the experimental micropore volume of 0.18 cm^3 g^{-1}. The predicted micropore volumes for the other carbon/silica composites were also in a qualitative agreement with those evaluated from nitrogen adsorption measurements.

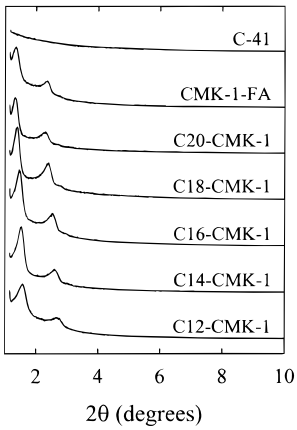

Figure 3. Powder X-ray diffraction patterns for the CMK-1 carbon molecular sieves and the MCM-41-templated carbon.

3.3. Carbons. *X-ray Diffraction.* Powder XRD patterns for the MCM-48-templated carbons (Figure 3) indicated long-range structural ordering, as reported before.[16,17] A relation between the crystallographic structures of MCM-48 and CMK-1, as well as the problem of CMK-1 structure assignment, was discussed in some detail elsewhere,[16] but further studies in this direction will be needed. MCM-41-templated carbon had a featureless XRD spectrum, as already reported by others.[18] This can be attributed to the fact that MCM-41 has disconnected channel-like pores,[18] and consequently the carbon deposit in MCM-41 is likely to consist of a honeycomb array of disconnected carbon rods. After removal of the MCM-41 template, such a nanostructure readily collapses.[18]

The CMK-1 unit-cell parameter can readily be tailored by choosing MCM-48 template of a proper unit-cell size. For instance, MCM-48 templates prepared using ionic surfactants of different alkyl chain lengths afforded carbons with unit-cell parameters from 8.0 to 9.4 nm (see Table 2). It should be noted

TABLE 2: Structural Properties of the Carbon Samples[a]

sample	a (nm)	S_{BET} ($m^2\ g^{-1}$)	V_t ($cm^3\ g^{-1}$)	V_p ($cm^3\ g^{-1}$)	S_{ex} ($m^2\ g^{-1}$)	w_{KJS} (nm)	w_{DFT} (nm)	residue (%)
C20-CMK-1	9.39	1710	1.23	1.02	60	3.4	2.9	4
C18-CMK-1	9.05	1800	1.21	1.08	60	3.4	2.9	2
C16-CMK-1	8.61	1700	1.24	1.02	110	3.4	2.9	2
C14-CMK-1	8.12	1560	1.07	0.96	60	3.4	3.0	3
C12-CMK-1	8.00	1740	1.12	1.03	40	3.3	2.9	3
CMK-1-FA	9.25	1560	1.08	0.91	80	3.4	2.9	3
C-41	*b*	1170	0.67	0.50	70	*c*	*c*	10

[a] a, XRD unit cell parameter equal to $2^{1/2}d_{110}$; w_{DFT}, maximum of the DFT pore size distribution peak in the mesopore range (above 2 nm). Residue, TGA residue at 1260 K under air atmosphere. For other notation, see Table 1. [b] Featureless XRD spectrum. [c] Pore size distribution primarily in the micropore range (below 2 nm).

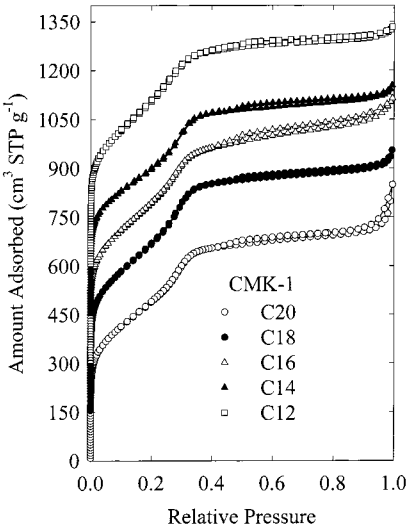

Figure 4. Nitrogen adsorption isotherms for the C*n*-CMK-1 carbon molecular sieves. The adsorption data for C18-, C16-, C14-, and C12-CMK-1 were offset vertically by 150, 300, 450, and 600 cm^3(STP) g^{-1}, respectively.

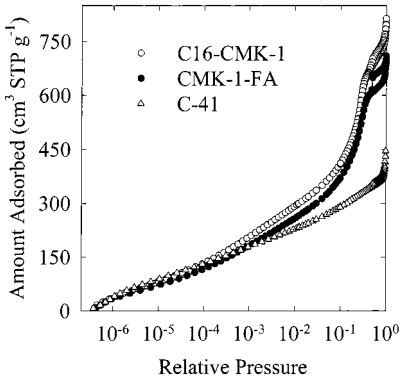

Figure 5. Low-pressure nitrogen adsorption isotherms for the C16-CMK-1, CMK-1 synthesized using furfuryl alcohol and MCM-41-templated carbon.

that the dissolution of MCM-48 template did not result in any appreciable change of the unit cell parameter. As reported before,[16,17] the synthesis of ordered carbon molecular sieves using MCM-48 templates is flexible in terms of carbon precursors used. For instance, the carbon prepared using furfuryl alcohol instead of sucrose exhibited good structural ordering (see Figure 3). Despite the use of the template with a moderate unit-cell size (C16-MCM-48), CMK-1-FA had a relatively large unit-cell size, which may be related to a low thermal shrinkage of the aluminosilicate template used for its synthesis.

Nitrogen Adsorption. The CMK-1 samples had large BET specific surface areas (about 1700 $m^2\ g^{-1}$) and large primary pore volumes (1 $cm^3\ g^{-1}$) (see Table 2). As discussed elsewhere,[39] the nitrogen BET method severely overestimates the specific surface area of carbons with relatively narrow pores. Therefore, the nitrogen BET surface areas provided here are most likely overestimated and the actual specific surface areas are probably much closer to that reported before (about 1400 $m^2\ g^{-1}$)[16] on the basis of argon BET analysis.

Similarly to the argon adsorption results reported before,[16] the nitrogen adsorption isotherms of the CMK-1 samples (Figures 2 and 4) featured steps at relative pressures of about 0.3, which can be attributed to capillary condensation in the ordered mesoporous structure. The capillary condensation steps for C20-, C18-, C16-, and C14−CMK-1 were clearly pronounced. To our best knowledge, such a behavior has not been reported for any other kind of carbons with micropores and/or narrow mesopores. The carbons reported before exhibited adsorption isotherms (plotted in the normal scale) which gradually increased as the pressure increased.[39−41] We found only one case where the nitrogen adsorption isotherm for a carbon with narrow pores exhibited some evidence of a stepwise behavior (when plotted in the normal scale) [41] but the step was poorly pronounced and broad. One can conclude that adsorption isotherms provided evidence of exceptionally narrow mesopore size distributions for the CMK-1 samples, when compared to the carbons reported before.

As can be inferred from the similarity in the shape of high-pressure hysteresis loops for the Cn-MCM-48 and Cn-CMK-1 samples under study, CMK-1 carbons exhibited secondary mesoporosity similar to that of the siliceous templates used for their synthesis. This suggests the retention of the secondary pore shape. The preservation of particle's morphology on somewhat larger length scale has already been demonstrated using scanning electron microscopy.[16] Only C16-CMK-1 had unexpectedly large external surface area and secondary pore volume, which may be indicative of the breakage of the carbon framework into smaller fragments during the silica template dissolution.

In contrast to the adsorption behavior of CMK-1, nitrogen adsorption of MCM-41-templated carbon did not provide any indications of a uniform mesoporous structure.[18] Indeed, this adsorption isotherm was similar to those observed for microporous carbons (see for instance refs 39−41). The MCM-41-templated carbon also exhibited much lower BET specific surface area and pore volume in comparison to those typical for CMK-1. Shown in Figure 5 are low-pressure adsorption isotherms for the CMK-1 samples and the MCM-41-templated carbon. The CMK-1 materials exhibited very similar low-pressure behavior (as illustrated for C16-CMK-1 and CMK-1-FA), despite the fact that they were prepared using two different carbon sources (sucrose and furfuryl alcohol). The adsorption isotherms for CMK-1 shown in the logarithmic scale exhibited a shape intermediate between that commonly observed for silicas, such as MCM-48[21] or MCM-41,[23,28] and that for typical

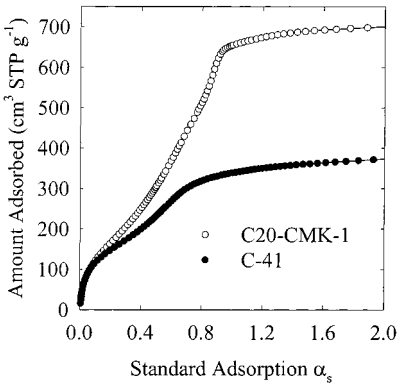

Figure 6. α_s plots for the C20-CMK-1 carbon molecular sieve and MCM-41-templated carbon.

porous carbons, such as activated carbons and carbon blacks.[39] Namely, there was some indication of a weakly-pronounced monolayer formation step at relative pressures of about 0.001−0.01. There is no such a step on adsorption isotherms for silicas, whereas the monolayer formation step is usually clearly pronounced for porous carbons. This behavior may result from a strong heterogeneity of CMK-1 surface or from a broad distribution of micropores.

The α_s plots for the CMK-1 samples were indicative of microporosity, since they exhibited initial upward deviations from the linear behavior, which are characteristic of microporous carbons (see Figure 6).[35,39−41] One can often estimate the micropore volume using the α_s plot analysis, but in the case of CMK-1, the presence of relatively narrow mesopores and the possible differences in surface properties between these carbons and the reference adsorbents available would render such an estimation unreliable.

The low-pressure adsorption isotherm (Figure 5) and the α_s plot (Figure 6) for the MCM-41-templated carbon were generally similar to those for conventional microporous carbons.[39] Thus, similarly to microporous carbons prepared using zeolitic templates,[11−13] this material was a high-surface-area carbon obtained without the need for activation, which is usually a mandatory step required for the development of well-accessible high-surface-area microporous carbon structure.[1,2] In contrast, a carbon sample prepared from sucrose without the application of the silica template exhibited exceptionally poor nitrogen adsorption properties, which manifested themselves in very slow equilibration and low nitrogen gas uptake. It is thus clear that the use of the template was responsible for the development of facile adsorption properties of the microporous structure of the MCM-41-templated carbon. The nitrogen adsorption isotherm for the MCM-41-templated carbon (Figure 2) exhibited a pronounced hysteresis loop at relative pressures above about 0.5, indicating the presence of secondary porosity. Since the MCM-41 template did not exhibit such a behavior, and in fact had very low secondary pore volume, one can conclude that the secondary porosity of the MCM-41-templated carbon developed as a result of the collapse of the periodic carbon structure during the template removal.

The pore size of the CMK-1 samples was found to be independent of the unit-cell parameter of the MCM-48 templates (Tables 1 and 2), which manifested itself in the appearance of capillary condensation steps at very similar relative pressures (see Figures 2 and 4).

Structural Considerations. The observed invariance of the pore size of CMK-1 upon the unit-cell increase can be explained when one considers the possible structure of carbons templated by MCM-48 silicas. The interconnected pore structure of MCM-48 silica is known to be confined within the silica wall whose midplane is located on a periodic minimal surface.[42−44] The wall separates the pore structure into two pairs of enantiomeric channel systems. Consequently, the carbon framework formed within the MCM-48 pores is expected to consist of two disconnected enantiomeric systems separated by the silica wall. During the preparation of CMK-1, the silica wall is dissolved and thus the pore size for CMK-1 is likely to be related to the pore wall thickness of MCM-48. Using eq 1, the pore wall thickness was estimated to be similar for all the MCM-48 samples under study and equal to about 1 nm (see Table 1). In light of the recent single-crystal electron diffraction study of MCM-48, which provided an average pore wall thickness of 1.3 nm,[44] the values of about 1 nm obtained for the MCM-48 samples under study appear to be reasonable. The similarity in the pore wall thickness of the MCM-48 templates is likely to be the reason for the similarity in the pore size for the CMK-1 samples studied, but still does not provide an answer as to why this pore size is much larger than the pore wall thickness of MCM-48. The latter behavior can be understood on the basis of the following considerations.

The preparation of the carbon−silica composite involves a high-temperature treatment, which leads to a significant shrinkage of the structure, as already discussed. This shrinkage is likely to lead to a considerable silica wall thickening (from 0.96−1.03 to 1.18−1.32 nm in the case of the C*n* samples studied, as evaluated using eq 1 from the estimated pore volumes after shrinkage). Since CMK-1 is formed via dissolution of silica from the carbon−silica composite, the space where the silica wall was once located is likely to constitute the primary pores of CMK-1 and thus the width of these pores would be at least about 1.18−1.32 nm. It also needs to be kept in mind that the micropores present in the carbon−silica composites may be located between the silica template and the carbon framework formed, thereby further increasing the distance between the adjacent parts of the carbon framework. In addition, the templated carbon is expected to have two separate framework systems. The possible collapse of them on one another may be prevented by a structural transformation upon MCM-48 template removal, which would relieve the frustration or strain of the carbon structure formed under the harsh pyrolysis conditions in the confined environment of the MCM-48 pores.[16] This transformation would lead to a situation where the two disconnected interwoven CMK-1 framework systems would have some sort of contact with one another, which would fix their mutual position. XRD spectra for the CMK-1 carbons clearly indicated that the periodic structure of CMK-1 was somewhat different from that of MCM-48,[16] which may be related to the displacement of the two CMK-1 framework systems with respect to one another as a result of the aforementioned structural transformation. It should be noted that the analysis of the recently published data for HMS-templated SNU-2 carbon[18] suggests that the large pore size of CMK-1 is not related primarily to the structural transformation, which takes place during CMK-1 synthesis. That is, SNU-2 carbon had only slightly smaller pore size when compared to CMK-1 (as inferred from the position of capillary condensation steps on the nitrogen adsorption isotherms; see ref 18 and the data reported therein). The pore wall thickness of HMS template is expected to be similar to that for MCM-41 (about 1 nm[23,34]) and thus comparable to that of MCM-48. Therefore, the general similarity in the pore size of CMK-1 and SNU-2 appears to be related to their similar pore wall thickness and indicates that the structural

transformation during the CMK-1 synthesis does not have any major influence on the pore size of CMK-1. This in turn suggests that the distance between the silica template wall and the templated carbon structure may provide a major contribution to the pore size of the templated mesoporous carbons. Anyway, further studies of CMK-1 structure and the nature of the transformation which accompanies the silica template dissolution will be required to fully understand the nature of the mesoporosity of these novel carbons.

It is interesting to note here that it is possible to predict the primary pore volume of CMK-1 on the basis of the pore volume of the calcined MCM-48 template, and contents of carbon and silica in the structure. It was already discussed how to predict the pore (micropore) volume in the carbon−silica composites. This reasoning can be extended by assuming that the volume of the MCM-48 walls additionally contributes to the primary pore volume of the resulting carbon. After recalculation for the unit mass of carbon in the structure, the sum of the micropore volume of the carbon−silica composite and the volume of the silica walls provides an estimate of the primary pore volume. For instance, in the case of C18-CMK-1, 1 g of carbon/silica composite is predicted to exhibit the micropore volume of 0.14 cm^3 and it contains 0.55 g of silica, which occupies the volume of 0.55 g/2.2 g cm^{-3} = 0.25 cm^3. Since 1 g of this composite contains 0.38 g of carbon, the volume of silica and micropores per 1 g of carbon is equal to (0.25 cm^3 + 0.14 cm^3)/0.38 g = 1.00 cm^3 g^{-1}, which is close to the value of 1.08 cm^3 g^{-1} obtained experimentally for C18-CMK-1. The estimates for other C*n*-CMK-1 samples differed from the actual ones by 8−24%, which is quite remarkable taking into consideration that the development of the porous structure of CMK-1 is still not fully understood.

Since the primary mesopores of CMK-1 are most likely formed in place of the MCM-48 pore walls, the latter being located in the midplane of a periodic minimal surface, these pores are probably more slitlike than cylindrical. Thus, the evaluation of their size using the DFT software for carbons with slitlike pores (see Table 2) is likely to be more accurate than that obtained using a procedure calibrated for cylindrical pores. The DFT-based pore sizes were essentially the same for all the CMK-1 samples considered and equal to about 2.9 nm. This value is larger than that estimated from the MCM-48 pore wall thickness in the carbon−silica composite (about 1.25 nm). However, as discussed above, the latter value does not account for the possible contribution of the distance between the MCM-48 pore wall and the templated carbon structure, not to mention the possible effect of the structural transformation that accompanies the MCM-48 template removal.

Thermogravimetry. Thermogravimetric weight changes recorded under air (or in general, oxygen-containing) atmosphere are commonly used to study homogeneity and phase purity of carbons, including nanotubes,[45,46] and carbons prepared using microporous materials as templates.[13] Therefore, it was interesting to verify whether this simple and highly useful methodology can be extended on carbons templated using ordered mesoporous silicas. As can be seen in Figures 7 and 8, the CMK-1 samples under study exhibited generally similar weight change patterns under air atmosphere. That is, there was usually a significant weight loss in a narrow temperature range somewhere between 650 and 725 K. This temperature is much lower than that reported for nanotubes and other graphitized carbons,[45,46] which provided a confirmation of a nongraphitized nature of CMK-1 framework. The temperature corresponding to the prominent weight loss for CMK-1 had a tendency to increase as the unit-cell size of the sample increased. Although the details of the CMK-1 pore wall structure and pore geometry have not been fully elucidated, it is justified to assume that the unit-cell size of CMK-1 increases as its pore size and pore wall thickness increase. Since the pore size of the CMK-1 materials under study is relatively constant, the increase in the unit-cell dimensions is likely to be related to the increased pore wall thickness. Therefore, the observed differences in the thermal stability may be related to the larger pore wall thickness for the CMK-1 materials with larger unit-cell sizes. However, the CMK-1 pore wall thickness is not likely to be the only factor determining the stability in the oxygen-containing atmosphere, because C20-CMK-1 and CMK-1-FA samples were not particularly stable,

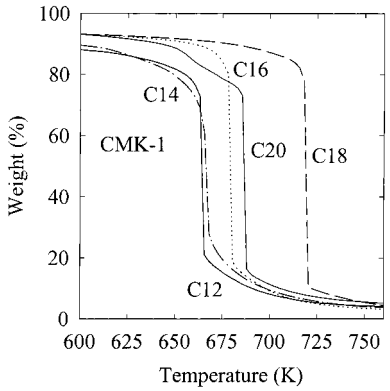

Figure 7. High-resolution thermogravimetric weight change curves under air atmosphere for the C*n*-CMK-1 carbon molecular sieves.

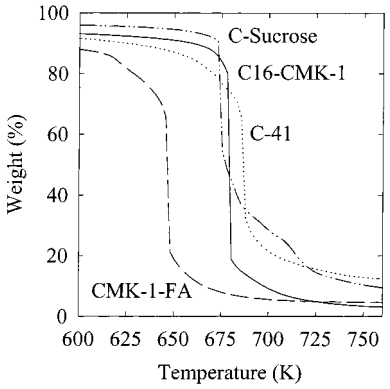

Figure 8. Comparison of high-resolution thermogravimetric weight change curves under air atmosphere for the C16-CMK-1 and CMK-1-FA carbon molecular sieves, MCM-41-templated carbon and carbon prepared via carbonization of pure sucrose.

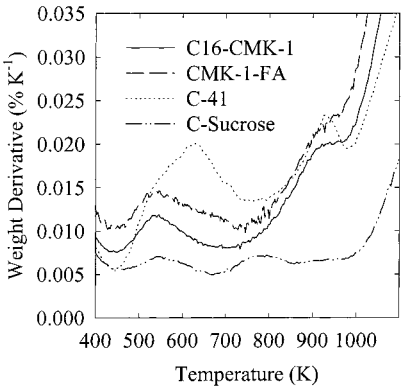

Figure 9. Comparison of high-resolution thermogravimetric weight change derivatives under nitrogen atmosphere for the C16-CMK-1 and CMK-1-FA carbon molecular sieves, MCM-41-templated carbon and carbon prepared via carbonization of pure sucrose.

despite their relatively large pore wall thicknesses expected on the basis of the large unit-cell sizes. For CMK-1-FA, the lower stability may be related to the application of furfuryl alcohol as a carbon precursor, which may render a less stable carbon framework, in addition to its lower structural ordering, which was reported elsewhere.[16] For C20-CMK-1, the weight change pattern featured an additional lower-temperature weight loss region at 650−690 K, which may be related to heterogeneity of the structure of the carbon framework. This heterogeneity may lower an overall thermal stability of the structure, similarly to the case of single-wall carbon nanotubes contaminated with less stable forms of carbon.[46]

It is also interesting to note that the C18-CMK-1 sample, which was the most stable in air and exhibited the highest percentage of the weight loss in a narrow temperature range in compared to other CMK-1 samples, exhibited the highest primary pore volume and surface area. Moreover, C14-CMK-1 and CMK-1-FA samples, which had the lowest specific surface areas and primary pore volumes, exhibited relatively low decomposition/oxidation temperatures, and relatively large weight losses at temperatures preceding and following the narrow region of the significant weight loss. The low combustion temperature as well as the weight loss preceding the primary combustion region may be related to the presence of structural defects in the CMK-1 framework, which would make it weaker and more prone to oxidation. These defects may form during the removal of the template, since the carbon/silica composites exhibited highly similar temperatures of carbon combustion. The weight loss at temperatures higher than those corresponding to the primary decomposition/oxidation region may possibly result from the existence of dense carbon deposits,[13] possibly on the external surface of CMK-1, although the previous TEM studies of CMK-1 samples did not indicate the presence of such deposits.[16] It is also interesting that in comparison to the CMK-1 samples, both MCM-41-templated carbon and the carbon prepared without a template exhibited broader ranges of combustion temperatures and lower weight losses in narrow primary decomposition/oxidation regions. One can conclude that the structural homogeneity of CMK-1 samples can be judged on the basis of weight change patterns in an oxygen-containing atmosphere. It should also be noted that MCM-41-templated carbon exhibited relatively large residue at 1260 K (10%), which was probably related to the difficulty in the quantitative removal of the template from the carbon matrix prone to the structural collapse. The CMK-1 carbons had much lower residues (2−4%), indicating that in this case the silica template can be removed to a significant extent from the carbon structure.

Some additional insight into structural properties of the carbons under study can be gained from the weight change curves recorded under nitrogen atmosphere (Figure 9). The latter provide information about decomposition of surface groups as well as the stability of carbon material in non-oxidative atmosphere.[47,48] The carbons under study exhibited only minor weight losses at temperatures below about 900 K, and the residues at 1260 K were larger than 83%, which shows that these carbons were much more stable in non-oxidative atmosphere than in the oxygen-rich atmosphere. The weight change patterns for CMK-1 samples were similar independently from the unit-cell size and the carbon precursor used, whereas the MCM-41-templated carbon and nontemplated carbon exhibited somewhat different weight change behaviors. This indicates that the CMK-1 carbons had similar surface groups, while the other two carbons had somewhat different surface functionalities. This in turn suggests that the templating and the effects of the template removal may have an impact not only on the porous properties of carbons but also on their surface functionality and thermal stability.

4. Conclusions

The current study demonstrated that the unit-cell size of CMK-1 mesoporous carbons can be tailored by choosing the MCM-48 template of an appropriate unit-cell dimension. However, the pore size of the resulting materials is quite independent of the unit-cell size and may possibly be tailored by using MCM-48 templates with different pore wall thickness. The application of a template with a three-dimensional interconnected channel system is crucial in the synthesis of periodic carbon frameworks. Carbons synthesized under otherwise identical conditions without a template or using a template with one-dimensional pores were found to be microporous. However, in this case, the templating was also beneficial because it resulted in the development of the structure with better micropore accessibility and relatively high specific surface area. It was shown that the pore volume of the CMK-1 carbons can be qualitatively predicted on the basis of the pore volume of MCM-48 templates, the unit-cell-size decrease upon carbonization, and the carbon content in carbon−silica composite materials. It was also demonstrated that weight change behavior in air atmosphere is correlated with the structure and adsorption capacity of the templated carbons, thus providing the means for a qualitative assessment of the structural homogeneity of CMK-1 carbons.

Acknowledgment. The donors of the Petroleum Research Fund administrated by the American Chemical Society are gratefully acknowledged for a partial support of this research.

Supporting Information Available: Figure 1S with experimental XRD data. This material is available free of charge via the Internet at http://pubs.acs.org.

References and Notes

(1) Bansal, C. R.; Donnett, J.-B.; Stoeckli, F. *Active Carbon*; Marcel Dekker: New York, 1988.
(2) Jankowska, H.; Swiatkowski, A.; Choma, J. *Active Carbon*; Ellis Horwood: Chichester, UK, 1991.
(3) Heiley, P. A. *J. Phys. Chem. Solids* **1992**, *53*, 1333.
(4) Thess, A.; Lee, R.; Nikolaev, P.; Dai, H.; Petit, P.; Robert, J.; Xu, C.; Lee, Y. H.; Kim, S. G.; Rinzler, A. G.; Colbert, D. T.; Scuseria, G. E.; Tomanek, D.; Fischer, J. E.; Smalley, R. E. *Science* **1996**, *273*, 483.
(5) Martinez-Alonso, A.; Tascon, J. M. D.; Bottani, E. J. *Langmuir* **2000**, *16*, 1343.
(6) Yim, Y. F.; Mays, T.; McEnaney, B. *Langmuir* **1999**, *15*, 8714.
(7) Eswaramoorthy, M.; Sen, R.; Rao, C. N. R. *Chem. Phys. Lett.* **1999**, *304*, 207.
(8) Subramoney, S. *Adv. Mater.* **1998**, *10*, 1157.
(9) Zakhidov, A. A.; Baughman, R. H.; Iqbal, Z.; Cui, C.; Khayrullin, I.; Dantas, S. O.; Marti, J.; Ralchenko, V. G. *Science* **1998**, *282*, 897.
(10) Sing, K. S. W.; Everett, D. H.; Haul, R. A. W.; Moscou, L.; Pierotti, R. A.; Rouquerol, J.; Siemieniewska, T. *Pure Appl. Chem.* **1985**, *57*, 603.
(11) Kyotani, T.; Nagai, T.; Inoue, S.; Tomita, A. *Chem. Mater.* **1997**, *9*, 609.
(12) Johnson, S. A.; Brigham, E. S.; Ollivier, P. J.; Mallouk, T. E. *Chem. Mater.* **1997**, *9*, 2448.
(13) Rodriguez-Mirasol, J.; Cordero, T.; Radovic, L. R.; Rodriguez, J. J. *Chem. Mater.* **1998**, *10*, 550.
(14) Beck, J. S.; Vartuli, J. C.; Roth, W. J.; Leonowicz, M. E.; Kresge, C. T.; Schmitt, K. D.; Chu, C. T-W.; Olson, D. H.; Sheppard, E. W.; McCullen, S. B.; Higgins, J. B.; Schlenker, J. L. *J. Am. Chem. Soc.* **1992**, *114*, 10834.
(15) Morey, M. S.; Davidson, A.; Stucky, G. D. *J. Porous Mater.* **1998**, *5*, 195.
(16) Ryoo, R.; Joo, S. H.; Jun, S. *J. Phys. Chem. B* **1999**, *103*, 7743.
(17) Lee, J.; Yoon, S.; Hyeon, T.; Oh, S. M.; Kim, K. B. *Chem. Commun.* **1999**, 2177.
(18) Lee, J.; Yoon, S.; Oh, S. M.; Shin, C.-H.; Hyeon, T. *Adv. Mater.* **2000**, *12*, 359.
(19) Tanev, P. T.; Pinnavaia, T. J. *Science* **1995**, *267*, 865.

(20) Ryoo, R.; Joo, S. H.; Kim, J. M. *J. Phys. Chem. B* **1999**, *103*, 7435.
(21) Kruk, M.; Jaroniec, M.; Joo, S. H.; Ryoo, R. *Chem. Mater.* **2000**, *12*, 1414.
(22) Ryoo, R.; Ko, C. H.; Park, I.-S. *Chem. Commun.* **1999**, 1413.
(23) Kruk, M.; Jaroniec, M.; Sakamoto, Y.; Terasaki, O.; Ryoo, R.; Ko, C. H. *J. Phys. Chem. B* **2000**, *104*, 292.
(24) Ryoo, R.; Jun, S.; Kim, J. M.; Kim, M. J. *Chem. Commun.* **1997**, 2225.
(25) Kruk, M.; Jaroniec, M.; Ryoo, R.; Kim, J. M. *Microporous Mater.* **1997**, *12*, 93.
(26) Kruk, M.; Jaroniec, M.; Gadkaree, K. P. *J. Colloid Interface Sci.* **1997**, *192*, 250.
(27) Jaroniec, M.; Kruk, M.; Olivier, J. P. *Langmuir* **1999**, *15*, 5410.
(28) Kruk, M.; Jaroniec, M.; Sayari, A. *Langmuir* **1997**, *13*, 6267.
(29) Barrett, E. P.; Joyner, L. G.; Halenda, P. P. *J. Am. Chem. Soc.* **1951**, *73*, 373.
(30) Kruk, M.; Antochshuk, V.; Jaroniec, M.; Sayari, A. *J. Phys. Chem. B* **1999**, *103*, 10670.
(31) Olivier, J. P. *Carbon* **1998**, *36*, 1469.
(32) Ravikovitch, P. I.; Neimark, A. V. *Langmuir* **2000**, *16*, 2419.
(33) Iler, R. K. *The Chemistry of Silica*; Wiley: New York, 1979.
(34) Kruk, M.; Jaroniec, M.; Sayari, A. *J. Phys. Chem. B* **1997**, *101*, 583.
(35) Gregg, S. J.; Sing, K. S. W. *Adsorption, Surface Area and Porosity*; Academic Press: London, 1982.
(36) Chen, L. Y.; Jaenicke, S.; Chuah, G. K. *Microporous Mater.* **1997**, *12*, 323.
(37) Mokaya, R. *J. Phys. Chem. B* **1999**, *103*, 10204.
(38) Chen, L.; Horiuchi, T.; Mori, T.; Maeda, K. *J. Phys. Chem. B* **1999**, *103*, 1216.
(39) Kruk, M.; Jaroniec, M.; Gadkaree, K. P. *Langmuir* **1999**, *15*, 1442.
(40) Kenny, M.; Sing, K.; Theocharis, C. In *Fundamentals of Adsorption*; Suzuki, M., Ed.; Kodansha: Tokyo, 1993; p 323.
(41) Kaneko, K.; Ishii, C.; Rybolt, T. *Stud. Surf. Sci. Catal.* **1994**, *87*, 583.
(42) Monnier, A.; Schuth, F.; Huo, Q.; Kumar, D.; Margolese, D.; Maxwell, R. S.; Stucky, G. D.; Krishnamurty, M.; Petroff, P.; Firouzi, A.; Janicke, M.; Chmelka, B. F. *Science* **1993**, *261*, 1299.
(43) Alfredsson, V.; Anderson, M. W. *Chem. Mater.* **1996**, *8*, 1141.
(44) Carlsson, A.; Kaneda, M.; Sakamoto, Y.; Terasaki, O.; Ryoo, R.; Joo, S. H. *J. Electron Microsc.* **1999**, *48*, 795.
(45) Rinzler, A. G.; Liu, J.; Dai, H.; Nikolaev, P.; Huffman, C. B.; Rodriguez-Macias, F. J.; Boul, P. J.; Lu, A. H.; Heymann, D.; Colbert, D. T.; Lee, R. S.; Fischer, J. E.; Rao, A. M.; Eklund, P. C.; Smalley, R. E. *Appl. Phys. A* **1998**, *67*, 29.
(46) Dillon, A. C.; Gennett, T.; Jones, K. M.; Alleman, J. L.; Parilla, P. A.; Heben, M. J. *Adv. Mater.* **1999**, *11*, 1354.
(47) Choma, J.; Burakiewicz-Mortka, W.; Jaroniec, M.; Li, Z.; Klinik, J. *J. Colloid Interface Sci.* **1999**, *214*, 438.
(48) Kruk, M.; Jaroniec, M.; Betz, W. R. *Langmuir* **1999**, *15*, 1435.